



Spontaneous reheating of crystallizing lava

Alan G. Whittington^{1*} and Alexander Sehlke²¹Department of Earth and Planetary Sciences, University of Texas at San Antonio, San Antonio, Texas 78249, USA²NASA Ames Research Center/Bay Area Environmental Research Institute, Moffett Field, California 94035, USA

ABSTRACT

We show that recalescence, or spontaneous reheating of a cooling material due to rapid release of latent heat, can occur during disequilibrium crystallization of depolymerized Mg-rich melts. This can only happen at fast cooling rates, where the melt becomes undercooled by tens to hundreds of degrees before crystallization begins. Using a forward-looking infrared (FLIR) camera, we documented recalescence in pyroxene ($\text{Fe}, \text{Mg}\text{SiO}_3$) and komatiite lavas that initially cooled at $25\text{--}50\text{ }^{\circ}\text{C s}^{-1}$. Local heating at the crystallization front exceeds $150\text{ }^{\circ}\text{C}$ for the pyroxene and $10\text{ }^{\circ}\text{C}$ for komatiite and lasts for several seconds as the crystallization front migrates through. We determined the latent heat release by differential scanning calorimetry to be 440 J g^{-1} for pyroxene and 275 J g^{-1} for komatiite with a brief power output of $\sim 100\text{ W g}^{-1}$ or $\sim 300\text{ MW m}^{-3}$. Recalescence may be a widespread process in the solar system, particularly in lava fountains, and cooling histories of mafic pyroclasts should not be assumed *a priori* to be monotonic.

INTRODUCTION

Molten materials, from magma oceans to lava droplets, crystallize when they are cooled at slow to moderate rates (Fig. 1A, path 1). Latent heat released during crystallization typically slows, but does not halt, monotonic cooling. During rapid cooling, molten materials can become supercooled, i.e., they can exist below their liquidus without immediately crystallizing. These supercooled liquids can undergo rapid disequilibrium crystallization at temperatures far below those of the liquidus but still above those of the glass transition (Fig. 1A, path 3; Kirkpatrick, 1975). If latent heat is released faster than it can be removed by radiation or conduction, the material can spontaneously heat up through a phenomenon known as recalescence (Fig. 1A, path 2; Fig. 1B). At the highest cooling rates, the liquid will quench to glass, which retains the amorphous structure of the liquid but lacks its mobility (Fig. 1A, path 4).

Recalescence has long been known in iron and effectively limits the minimum grain size achievable in steel production (Yokota et al., 2004). Recalescence occurs in poor glass-forming liquids such as the alumina-yttria-lanthana system (e.g., Tangeman et al., 2007) and has been observed in levitated Mg_2SiO_4 liquids, where container-less synthesis allows rapid

undercooling without crystallization (Tangeman et al., 2001). The latter example is the only reported experimental observation we could find of recalescence in silicate melts, as most experimental cooling-rate studies are conducted at cooling rates that are too slow for latent heat to produce net heating; instead, cooling rates are simply buffered (e.g., Lofgren and Russell, 1986; Longhi, 1992; Vetere et al., 2013). However, two studies suggest that recalescence took place in natural silicate melts; recalescence was proposed as an explanation for the irregular thermal histories recorded at the base of basaltic lava flows (Keszthelyi, 1995) and, over a much longer time scale, magma heating through the release of latent heat from crystallization has been inferred to explain data from plagioclase-hosted melt inclusions in andesitic lavas, which show increasing temperatures at decreasing pressures as magma ascends toward the surface and degasses (Blundy et al., 2006).

Polymerized silicate melts, including window glass and rhyolitic lavas, can quench to glass easily without requiring rapid cooling as indicated by the dense obsidian cores of some thick and slow-cooling rhyolite flows (e.g., Fink, 1983), which prevents the release of significant latent heat and makes recalescence impossible. In general, more depolymerized melts are poorer glass-formers and are more likely to undergo recalescence during rapid disequilibrium crystallization. This suggests that ultramafic lavas

such as komatiites, which were more common early in Earth history (Arndt et al., 2008), may undergo this process, which would affect both their thermal and rheological history during emplacement.

Such considerations also extend to extraterrestrial environments. Depolymerized mafic lavas cover much of the lunar nearside as well as parts of every terrestrial planet, and mafic (and possibly ultramafic) lavas have been observed erupting on Jupiter's moon Io (e.g., McEwen et al., 1998). We conducted a series of experiments to investigate dynamic crystallization at large degrees of undercooling for two depolymerized silicate compositions, a simple pyroxene ($\text{Fe}_{0.39}\text{Mg}_{0.59}\text{SiO}_{3.00}$) and a more complex komatiite ($\text{Ca}_{0.18}\text{Mg}_{0.46}\text{Fe}_{0.17}\text{Al}_{0.22}\text{Ti}_{0.01}\text{Si}_{0.91}\text{O}_{3.00}$), for which we had previously determined thermal diffusivity to high temperature (Hofmeister et al., 2014; Sehlke et al., 2020), and we documented recalescence in both lavas.

METHODS

Glass Synthesis

Starting glasses were synthesized from oxide and carbonate powders with repeated cycles of fusion in a $\text{Pt}_{90}\text{Rh}_{10}$ crucible, splat-quenching on a copper plate, and grinding to ensure homogeneity.

Forward-Looking Infrared (FLIR) Imaging

We performed quantitative observations using a tripod-mounted FLIR Systems® T650sc with a 640×480 sensor array looking vertically downwards toward the sample from a distance of $\sim 1\text{ m}$. We melted a few grams of pyroxene glass in a $\text{Pt}_{90}\text{Rh}_{10}$ crucible in a muffle furnace at $1590\text{ }^{\circ}\text{C}$ and then placed it onto a graphite plate kept at $\sim 550\text{ }^{\circ}\text{C}$ with a hot plate to reduce heat flow out of the base of the crucible.

Differential Scanning Calorimetry (DSC)

Chips of $\sim 25\text{--}50\text{ mg}$ were heated above their liquidus and then cooled to room temperature in a Netzsch® 404F1 Pegasus differential scanning calorimeter. Heat flow was converted

*E-mail: alan.whittington@utsa.edu

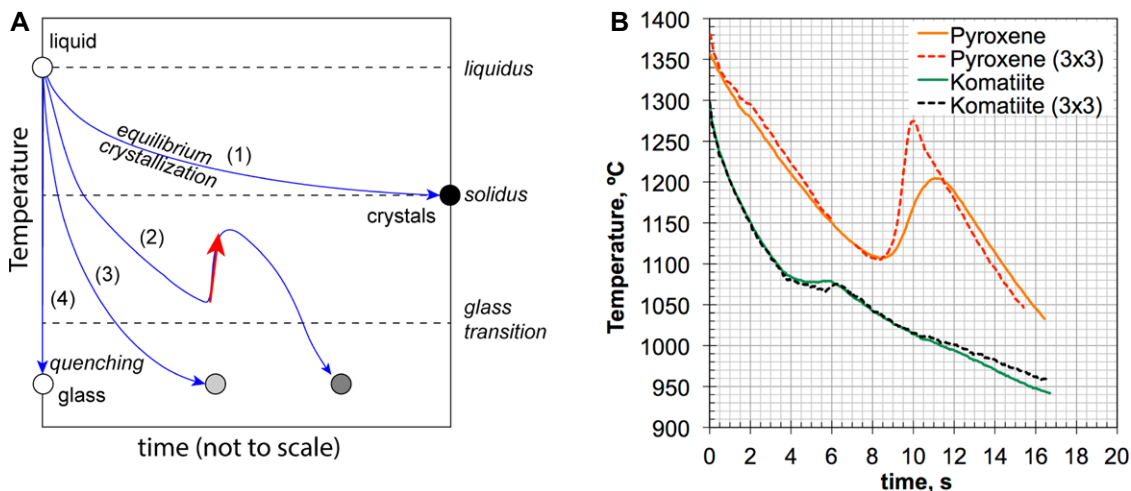


Figure 1. (A) Schematic temperature-time diagram. Numbered cooling paths are discussed in the text. Red arrow indicates recalescence. (B) Temperature-time diagram for lavas in our experiments. Solid lines average the entire crucible base ($\sim 19 \text{ cm}^2$), and dashed lines refer to 3×3 pixel areas ($\sim 1 \text{ mm}^2$).

to a quantitative measurement of isobaric heat capacity (C_p) by running a series of three experiments under identical temperature-time programs including heating at a constant rate, an isothermal dwell at high temperature, and cooling at a constant rate. The first experiment involved a blank (empty pan), the second a sapphire standard (Ditmars et al., 1982), and the third the material to be analyzed. Full details of experimental conditions and observed heat flow peaks are given in Table S1 in the Supplemental Material¹.

RESULTS

Crucible-Scale Cooling Experiments

Initial observations of recalescence were made during synthesis of some pyroxene melts $[(\text{Fe}, \text{Mg})\text{SiO}_3]$, when the crucible was removed from the furnace at $\sim 1600 \text{ }^\circ\text{C}$ and placed on a copper plate. During cooling, nucleating crystals appeared brighter than the surrounding melt. As they grew, the advancing crystallization fronts remained brightest, crystal interiors were less bright, and uncryallized melt was the least bright (Fig. 2; Video S1). These initial observations were recorded with a phone camera, which allowed only qualitative assessment of recalescence due to automatic brightness adjustments. We performed quantitative observations using a forward-looking infrared (FLIR) camera with an assumed emissivity of 0.95.

On cooling from $1590 \text{ }^\circ\text{C}$, at $\sim 30 \text{ }^\circ\text{C s}^{-1}$, crystallization of $\text{Fe}_{0.4}\text{Mg}_{0.6}\text{SiO}_3$ liquid begins at $\sim 1110 \text{ }^\circ\text{C}$, which is $\sim 370 \text{ }^\circ\text{C}$ below the liquidus temperature of $1480 \text{ }^\circ\text{C}$ (Muan and Osborn, 1956). Averaging over the whole base of the crucible ($\sim 10 \text{ cm}^2$), the observed temperature increase during crystallization was $\sim 100 \text{ }^\circ\text{C}$,

and it took $\sim 2.5 \text{ s}$ to attain the thermal peak (Fig. 1B). Crystallization and heating can be seen migrating across the melt volume together (Video S2). The hottest part of the image is always the crystallization front, where the latent heat is actually being released. The crystals are therefore always warmer than the melt because the crystallization front has already moved through them. Examining a 3×3 pixel spot ($\sim 1 \text{ mm}^2$ in our setup), reheating to $T > 1270 \text{ }^\circ\text{C}$ occurred in $\sim 1 \text{ s}$ (Fig. 1B). Recovered samples show the growth of needle-like spinifex-textured bronzite ($\text{Fe}_{0.20}\text{Mg}_{0.82}\text{Si}_{0.98}\text{O}_3$) with interstitial, iron-rich pyroxene crystals ranging in composition from ferrosilite ($\text{Fe}_{0.92}\text{Mg}_{0.10}\text{Si}_{0.97}\text{O}_3$) to ferrohypersthene ($\text{Fe}_{0.74}\text{Mg}_{0.25}\text{Si}_{0.99}\text{O}_3$); this range probably resulted from variable local Mg-depletion following early bronzite crystallization (Fig. 3; Table S1).

Upon cooling of komatiite liquid from $\sim 1590 \text{ }^\circ\text{C}$, the sample quenched to glass. Starting instead with the crucible at $\sim 1450 \text{ }^\circ\text{C}$ and cooling initially at $\sim 50 \text{ }^\circ\text{C s}^{-1}$, crystallization began at $\sim 1080 \text{ }^\circ\text{C}$. Averaging over the base of the crucible, cooling paused for $\sim 2 \text{ s}$ and then resumed at $\sim 15 \text{ }^\circ\text{C/min}$ (Fig. 1B). In a 3×3 pixel spot, $\sim 10 \text{ }^\circ\text{C}$ reheating occurred in $\sim 0.5 \text{ s}$. When viewed as the temperature difference between different video frames, newly formed crystals are $\sim 30 \text{ }^\circ\text{C}$ hotter than uncryallized melt, and crystallization mostly proceeded from the crucible wall to the interior of the melt (Fig. 1H). Recovered samples show small chrome spinel crystals surrounded by a dendritic intergrowth of aluminous, Mg-rich pigeonite ($\text{Ca}_{0.15}\text{Fe}_{0.14}\text{Mg}_{0.59}\text{Al}_{0.10}\text{Si}_{0.90}\text{O}_3$) and aluminous augite ($\text{Ca}_{0.25}\text{Fe}_{0.17}\text{Mg}_{0.38}\text{Al}_{0.11}\text{Si}_{0.91}\text{O}_3$) (Fig. 3). Komatiite lavas typically crystallize olivine first and often display spinifex texture with interstitial plagioclase and aluminous clinopyroxene (Shore and Fowler, 1999), but cooling rates in our experiments were fast enough to crystallize two pyroxenes instead in a metastable manner.

Differential Scanning Calorimetry Experiments

We also investigated crystallization using differential scanning calorimetry (DSC) to demonstrate that recalescence also occurs in melt quantities that are smaller by orders of magnitude and to quantify the heat flows involved. Samples were heated to a fully molten state at $\sim 1500 \text{ }^\circ\text{C}$ and then cooled at controlled rates of $50 \text{ }^\circ\text{C min}^{-1}$ or $100 \text{ }^\circ\text{C min}^{-1}$ to $500 \text{ }^\circ\text{C}$, which is well below their glass transition temperature (T_g). For pyroxene melt that was cooled at $\sim 50 \text{ }^\circ\text{C min}^{-1}$, two distinct crystallization peaks were seen at $1316 \text{ }^\circ\text{C}$ and $1264 \text{ }^\circ\text{C}$ (Fig. 4). During cooling, the enthalpy of crystallization appears as an increase in apparent heat capacity because the calorimeter must remove both the sensible and latent heat components.

Cooled at $\sim 100 \text{ }^\circ\text{C min}^{-1}$, a large peak was seen at $1313 \text{ }^\circ\text{C}$ with a smaller second peak at $1273 \text{ }^\circ\text{C}$. Examination of recovered samples indicates crystallization of bronzite ($\text{Fe}_{0.22}\text{Mg}_{0.84}\text{Si}_{0.97}\text{O}_3$) of a similar composition but much larger size than was observed in the FLIR experiment, with small ferrosilite crystals ($\text{Fe}_{0.94}\text{Mg}_{0.05}\text{Si}_{0.99}\text{O}_3$) and exsolution of silicarich melt globules ($\sim 97 \text{ wt\% SiO}_2$) interspersed within a more iron-rich, glassy matrix (Fig. 3). We interpret the first DSC peak as recording bronzite crystallization and the second as recording oxide growth. The total latent heat release is 472 J g^{-1} at $100 \text{ }^\circ\text{C/min}$ and 418 J g^{-1} , 439 J g^{-1} , and 484 J g^{-1} in three experiments at $50 \text{ }^\circ\text{C min}^{-1}$.

For komatiite melt cooled at $50 \text{ }^\circ\text{C min}^{-1}$, two distinct crystallization peaks were seen at $1139 \text{ }^\circ\text{C}$ and $986 \text{ }^\circ\text{C}$ (Fig. 4). Cooled at $\sim 100 \text{ }^\circ\text{C min}^{-1}$, the first peak was at $\sim 1125 \text{ }^\circ\text{C}$ while the second peak occurred at $\sim 1075 \text{ }^\circ\text{C}$. Examination of samples recovered indicates crystallization of forsteritic olivine needles ($\text{Fe}_{0.21}\text{Mg}_{1.76}\text{Si}_{1.00}\text{O}_4$) that in places adopt a graphic texture; numerous small ($\sim 2 \mu\text{m}$) magnetite crystals are concentrated on olivine faces, and there is a matrix of

¹Supplemental Material. Two supplemental tables and four videos. Please visit <https://doi.org/10.1130/GEOLOGICALSOCIETY.15078957> to access the supplemental material, and contact editing@geosociety.org with any questions.

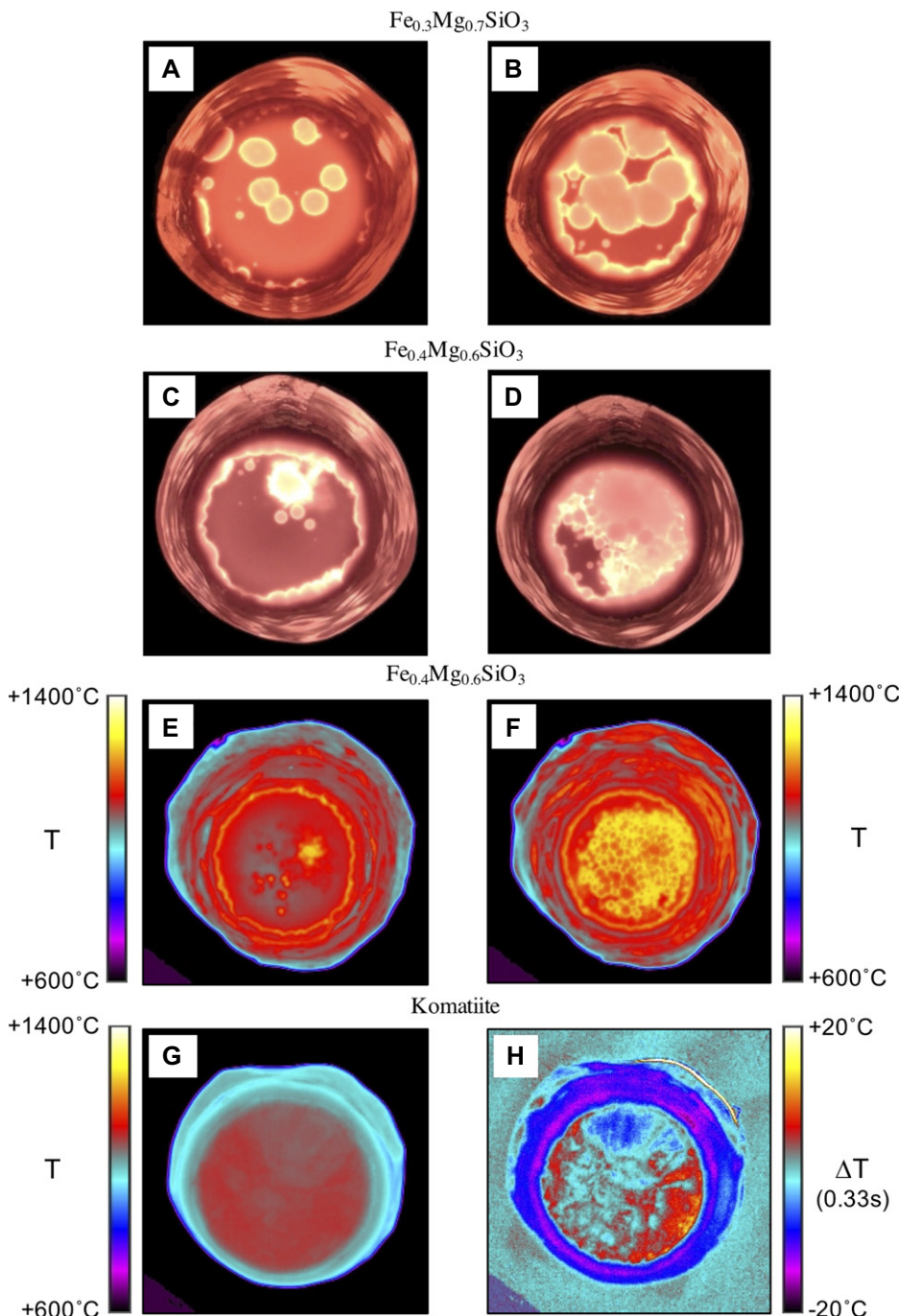


Figure 2. Images showing crystallizing silicate melts; A–D were taken by phone camera and E–G by forward-looking infrared (FLIR) camera. (A, B) $\text{Fe}_{0.3}\text{Mg}_{0.7}\text{SiO}_3$ and (C, D) $\text{Fe}_{0.4}\text{Mg}_{0.6}\text{SiO}_3$ liquids during cooling in Pt–Rh crucible; diameter at rim is ~ 7 cm and ~ 5 cm at base. (E, F) $\text{Fe}_{0.4}\text{Mg}_{0.6}\text{SiO}_3$ liquids. (G) Komatiite liquid. (H) Temperature change over a 0.33 s interval for komatiite liquid.

~ 10 - μm -sized dendritic aluminous augite ($\text{Ca}_{0.30}\text{Fe}_{0.19}\text{Mg}_{0.23}\text{Al}_{0.26}\text{Si}_{0.92}\text{O}_3$) similar in composition to the interstitial glass (Table S1). X-ray diffraction (XRD) analysis suggests the proportions of crystalline phases are ~ 55 wt% forsterite, ~ 40 wt% augite, and ~ 5 wt% magnetite. We interpret the larger, higher temperature DSC peak as recording olivine crystallization and the subsequent peak as recording augite growth. The ΔH^{xtal} for komatiite liquids was -233 J g^{-1} to

-293 J g^{-1} , which is lower than for the pyroxene liquids, because komatiitic liquids are more polymerized.

DISCUSSION

Our observations of reheating in excess of 100°C during spontaneous crystallization of depolymerized mafic melts have several implications for both terrestrial and planetary volcanology.

Temperature and Thermal History of Lava Flows and Lava Lakes

Indirect evidence for recalescence occurring in nature comes from observations of temperature fluctuations at the base of a basaltic lava flow at Kīlauea volcano, Hawai‘i (Keszthelyi, 1995). Our observations of temperature differences of up to $\sim 100^\circ\text{C}$ on a millimeter scale (Fig. 2) suggest that thermal imaging of basaltic lava flows using hand-held or tripod-mounted FLIR cameras needs to be conducted with millimeter-scale spatial resolution to assess true temperature fluctuations. Due to safety considerations, field-based temperature measurements of active lava flows and lakes are typically recorded from a distance that provides meter- to decimeter-scale rather than millimeter-scale spatial resolution (e.g., Harris et al., 2005; Spampinato et al., 2008; Harris, 2013), which may result in averaging cooler melt and hotter crystals within a single pixel and systematic overestimation of the temperature of the liquid phase.

In practice, radiative cooling is fast, and overestimating the melt temperature in a lava flow is unlikely. Wright and Flynn (2003) obtained FLIR images of pahoehoe flows at Kīlauea with ~ 4 mm spatial resolution, probably the highest to date, and found that the highest temperature pixel was only 1094°C , which is substantially cooler than temperatures inferred from the rheological behavior of Hawaiian lavas forming pahoehoe lobes (Sehlke et al., 2014). In a normal lava flow, each part of the flow surface only gets to cool once. In contrast, active lava lakes continually expose new batches of fresh, hot lava at the surface (e.g., Tilling, 1987). However, this lava may also cool too quickly for recalescence to occur, and active lava lakes are typically very difficult to approach closely enough to ensure millimeter-scale pixel sizes.

An alternative approach is to use numerical models of cooling and latent heat release, based on kinetic studies of crystal nucleation and growth rates, to predict recalescence (Keszthelyi, 1995). Thermal models of cooling lava that incorporate latent heat of crystallization as an “effective heat capacity” term, as is typically adopted for lava flows and cooling plutons (e.g., Nabelek et al., 2012; Harris, 2013), prohibit recalescence and may inaccurately capture the thermal history of rapidly cooling lava bodies.

Temperature and Thermal History of Lava Fountains

Droplets erupted in lava fountains can cool much more rapidly than larger bodies. Lava fountains on Earth typically involve tholeiitic basalts at shield volcanoes such as Kīlauea volcano (Eaton and Murata, 1960; Wolfe et al., 1987). Moitra et al. (2018) modeled cooling of basaltic pyroclasts and calculated cooling rates through 700°C ($\sim T_g$) of $\sim 3^\circ\text{C s}^{-1}$, 30°C s^{-1} , and 300°Cs^{-1} for clast diameters of 30 mm,

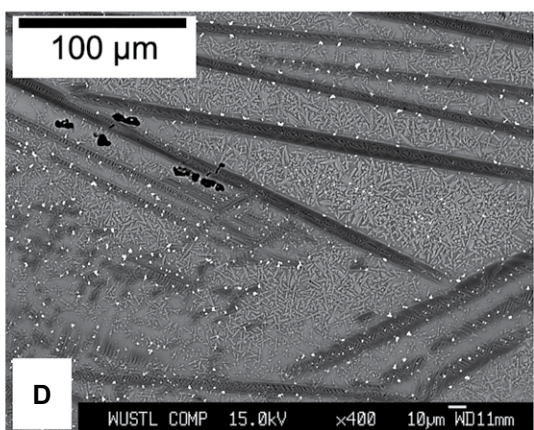
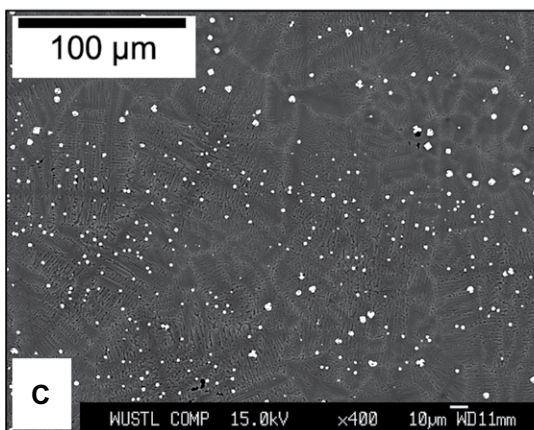
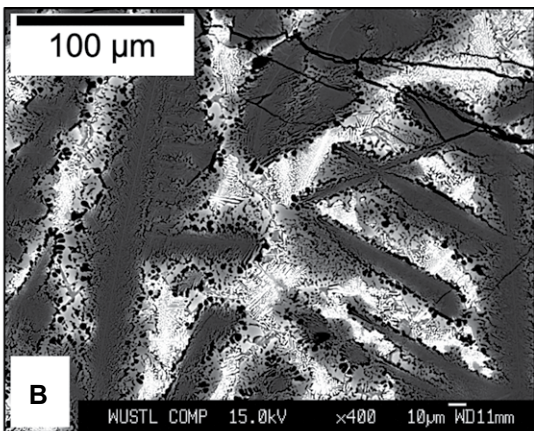
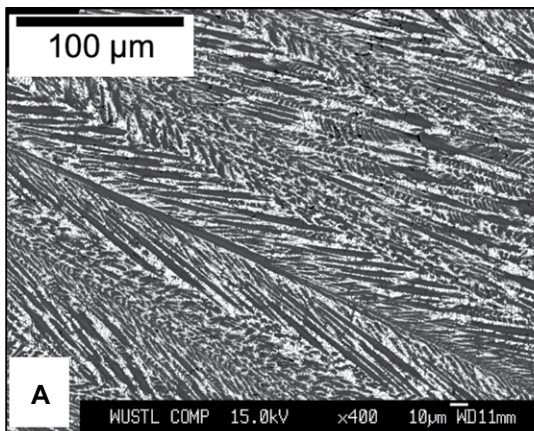


Figure 3. Textures of crystallized melts imaged using back-scattered electron microscopy: (A) $\text{Fe}_{0.4}\text{Mg}_{0.6}\text{SiO}_3$ melt in crucible, bronzite (dark gray), and ferrosilite (white). (B) $\text{Fe}_{0.4}\text{Mg}_{0.6}\text{SiO}_3$ melt in differential scanning calorimetry (DSC), bronzite (dark gray), ferrosilite (bright), silica-rich melt (black), and interstitial glass (medium gray). (C) Komatiite melt in crucible, chrome spinel (white), pigeonite (dark gray), and augite (light gray). (D) Komatiite melt in DSC, forsterite (dark gray), magnetite (white), augite (light gray), and interstitial glass (medium gray).

3 mm, and 0.3 mm, respectively, which suggests that coarse ash and small lapilli will typically cool at rates that are consistent with recrystallization in mafic melts. Volcanic glass spherules on the Moon are mostly <1 mm in size, but the larger spherules often contain acicular to fibrous crystals (Rutherford and Papale, 2009), textures

consistent with rapid disequilibrium crystallization, and perhaps with recrystallization (Fig. 3).

Active lava fountain events were observed on Jupiter's moon Io in November 1999 by NASA's Galileo mission (McEwen et al., 2000) and using ground-based telescopes over a 25 yr period (Davies, 1996; Stansberry et al., 1997; de Kleer

et al., 2019). These "outburst" eruptions have timescales similar to those of terrestrial events (hours to days). Ionian lavas were estimated to erupt at high temperatures, between 1200 and 1700 °C, based on observations by the Near-Infrared Mapping Spectrometer (NIMS) on the Galileo spacecraft (McEwen et al., 1998; Davies et al., 2000). Such high temperatures suggest mafic to ultramafic lava compositions such as komatiites.

Keszthelyi et al. (2007) modeled the thermal history of lava droplets on Io and predicted that 0.1 mm and 1 mm droplets would cool by ~ 650 °C and ~ 200 °C in 1 s. However, droplets were assumed to quench to glass in the models and were therefore unable to recrystallize and release heat during crystallization. Slightly larger droplets would cool in the ~ 50 °C s $^{-1}$ range of our cooling experiments, and they should recrystallize. In this case, the additional latent heat released will contribute to the overall thermal flux of the fountain but will not be accompanied by higher peak temperatures because recrystallization is limited to subliquidus temperatures (Fig. 1). Recrystallization would raise the temperatures of the hottest components, which are derived from model fits to observational data, closer to actual lava eruption temperatures. Hence, we would be closer to understanding the composition of silicate lavas erupting on Io.

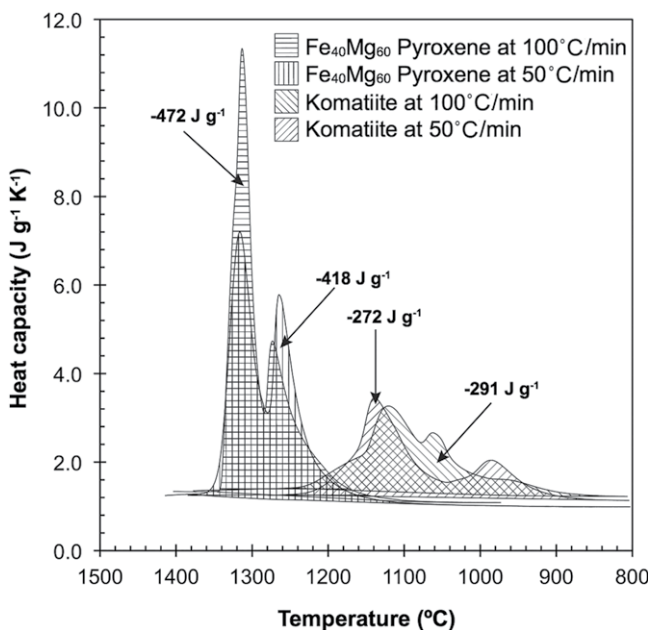


Figure 4. Apparent heat capacities measured using differential scanning calorimeter upon cooling from 1500 °C. Labeled enthalpies of crystallization are exothermic.

ACKNOWLEDGMENTS

We thank Jerry Beeney from FLIR systems (<https://www.flir.com>) for assisting with video acquisition, and Paul Carpenter for assistance with microprobe analysis. We thank Ashley Davies and an anonymous reviewer for comments that improved the manuscript. Funding for this work was provided by NASA grants NNX12AO44G and 80NSSC19K1010.

REFERENCES CITED

- Arndt, N.J., Lesser, C.M., and Barnes, S.J., 2008, *Komatiite*: Cambridge, UK, Cambridge University Press, 468 p., <https://doi.org/10.1017/CBO9780511535550>.
- Blundy, J., Cashman, K., and Humphreys, M., 2006, Magma heating by decompression-driven crystallization beneath andesite volcanoes: *Nature*, v. 443, p. 76–80, <https://doi.org/10.1038/nature05100>.
- Davies, A.G., 1996, Io's volcanism: Thermo-physical models of silicate lava compared with observations of thermal emission: *Icarus*, v. 124, p. 45–61, <https://doi.org/10.1006/icar.1996.0189>.
- Davies, A.G., Lopes-Gautier, R., Smythe, W.D., and Carlson, R.W., 2000, Silicate cooling model fits to Galileo NIMS data of volcanism on Io: *Icarus*, v. 148, p. 211–225, <https://doi.org/10.1006/icar.2000.6486>.
- de Kleer, K., et al., 2019, Io's volcanic activity from time domain adaptive optics observations: 2013–2018: *The Astronomical Journal*, v. 158, p. 29, <https://doi.org/10.3847/1538-3881/ab2380>.
- Dimars, D.A., Ishihara, S., Chang, S.S., Bernstein, G., and West, E.D., 1982, Enthalpy and heat capacity standard reference material: Synthetic sapphire (α -Al₂O₃) from 10 to 2250 K: *Journal of Research of the National Bureau of Standards*, v. 87, <https://doi.org/10.6028/jres.087.012>.
- Eaton, J.P., and Murata, K.J., 1960, How volcanoes grow: *Science*, v. 132, p. 925–938, <https://doi.org/10.1126/science.132.3432.925>.
- Fink, J.H., 1983, Structure and emplacement of a rhyolitic obsidian flow—Little Glass Mountain, Medicine Lake Highland, northern California: *Geological Society of America Bulletin*, v. 94, p. 362–380, [https://doi.org/10.1130/0016-7606\(1983\)94<362:SAEOAR>2.0.CO;2](https://doi.org/10.1130/0016-7606(1983)94<362:SAEOAR>2.0.CO;2).
- Harris, A.J.L., 2013, *Thermal Remote Sensing of Active Volcanoes: A User's Manual*: Cambridge, UK, Cambridge University Press, 728 p., <https://doi.org/10.1017/CBO9781139029346>.
- Harris, A.J.L., Dehn, J., Patrick, M., Calvari, S., Ripepe, M., and Lodato, L., 2005, Lava effusion rates from hand-held thermal infrared imagery: An example from the June 2003 effusive activity at Stromboli: *Bulletin of Volcanology*, v. 68, p. 107–117, <https://doi.org/10.1007/s00445-005-0425-7>.
- Hofmeister, A.M., Sehlke, A., and Whittington, A.G., 2014, Thermal diffusivity of Fe-rich pyroxene glasses and their melts: *Chemical Geology*, v. 384, p. 1–9, <https://doi.org/10.1016/j.chemgeo.2014.06.018>.
- Keszthelyi, L., 1995, Measurements of cooling at the base of pahoehoe flows: *Geophysical Research Letters*, v. 22, p. 2195–2198, <https://doi.org/10.1029/95GL01812>.
- Keszthelyi, L., Jaeger, W., Milazzo, M., Radebaugh, J., and Davies, A.G., 2007, New estimates for Io eruption temperatures: Implications for the interior: *Icarus*, v. 192, p. 491–502, <https://doi.org/10.1016/j.icarus.2007.07.008>.
- Kirkpatrick, R.J., 1975, Crystal growth from the melt: A review: *The American Mineralogist*, v. 60, p. 798–814.
- Lofgren, G.E., and Russell, W.J., 1986, Dynamic crystallization of chondrule melts of porphyritic and radial pyroxene composition: *Geochimica et Cosmochimica Acta*, v. 50, p. 1715–1726, [https://doi.org/10.1016/0016-7037\(86\)90133-X](https://doi.org/10.1016/0016-7037(86)90133-X).
- Longhi, J., 1992, Experimental petrology and petrogenesis of mare volcanics: *Geochimica et Cosmochimica Acta*, v. 56, p. 2235–2251, [https://doi.org/10.1016/0016-7037\(92\)90186-M](https://doi.org/10.1016/0016-7037(92)90186-M).
- McEwen, A.S., et al., 1998, High-temperature silicate volcanism on Jupiter's moon Io: *Science*, v. 281, p. 87–90, <https://doi.org/10.1126/science.281.5373.87>.
- McEwen, A.S., et al., 2000, Galileo at Io: Results from high-resolution imaging: *Science*, v. 288, p. 1193–1198, <https://doi.org/10.1126/science.288.5469.1193>.
- Moitra, P., Sonder, I., and Valentine, G.A., 2018, Effects of size and temperature-dependent thermal conductivity on the cooling of pyroclasts in air: *Geochemistry Geophysics Geosystems*, v. 19, p. 3623–3636, <https://doi.org/10.1029/2018GC007510>.
- Muan, A., and Osborn, E.F., 1956, Phase equilibria at liquidus temperatures in the system MgO-FeO-Fe₂O₃-SiO₂: *Journal of the American Ceramic Society*, v. 39, p. 121–140, <https://doi.org/10.1111/j.1151-2916.1956.tb14178.x>.
- Nabelek, P.I., Whittington, A.G., and Hofmeister, A.M., 2012, The influence of temperature-dependent thermal diffusivity on the conductive cooling rates of plutons and temperature-time paths in contact aureoles: *Earth and Planetary Science Letters*, v. 317–318, p. 157–164, <https://doi.org/10.1016/j.epsl.2011.11.009>.
- Rutherford, M.J., and Papale, P., 2009, Origin of basalt fire-fountain eruptions on Earth versus the Moon: *Geology*, v. 37, p. 219–222, <https://doi.org/10.1130/G25402A.1>.
- Sehlke, A., Whittington, A.G., Robert, B., Harris, A.J.L., Gurioli, L., and Médard, E., 2014, Pahoehoe to 'aa transition of Hawaiian lavas: An experimental study: *Bulletin of Volcanology*, v. 76, p. 876, <https://doi.org/10.1007/s00445-014-0876-9>.
- Sehlke, A., Hofmeister, A.M., and Whittington, A.G., 2020, Thermal properties of glassy and molten planetary candidate lavas: *Planetary and Space Science*, v. 193, <https://doi.org/10.1016/j.pss.2020.105089>.
- Shore, M., and Fowler, A.D., 1999, The origin of spinifex texture in komatiites: *Nature*, v. 397, p. 691–694, <https://doi.org/10.1038/17794>.
- Spampinato, L., Oppenheimer, C., Calvari, S., Cannata, A., and Montalto, P., 2008, Lava lake surface characterization by thermal imaging: Ertá 'Ale volcano (Ethiopia): *Geochemistry Geophysics Geosystems*, v. 9, Q12008, <https://doi.org/10.1029/2008GC002164>.
- Stansberry, J.A., Spencer, J.R., Howell, R.R., Dumas, C., and Vakil, D., 1997, Violent silicate volcanism on Io in 1996: *Geophysical Research Letters*, v. 24, p. 2455–2458, <https://doi.org/10.1029/97GL02593>.
- Tangeman, J.A., Phillips, B.L., Navrotzky, A., Weber, J.K.R., Hixson, A.D., and Key, T.S., 2001, Vitreous forsterite (Mg₂SiO₄): Synthesis, structure and thermochemistry: *Geophysical Research Letters*, v. 28, p. 2517–2520, <https://doi.org/10.1029/2000GL012222>.
- Tangeman, J.A., Phillips, B.L., and Hart, R., 2007, Nucleation of perovskite nanocrystals in a levitating liquid: *Journal of the American Ceramic Society*, v. 90, p. 758–762, <https://doi.org/10.1111/j.1551-2916.2007.01489.x>.
- Tilling, R.I., 1987, Fluctuations in surface height of active lava lakes during 1972–1974 Mauna Ulu Eruption, Kilauea Volcano, Hawaii: *Journal of Geophysical Research: Solid Earth*, v. 92, p. 13721–13730, <https://doi.org/10.1029/JB092iB13p13721>.
- Vetere, F., Iezzi, G., Behrens, H., Cavallo, A., Misiti, V., Dietrich, M., and Knipping, J., 2013, Intrinsic solidification behaviour of basaltic to rhyolitic melts: A cooling rate experimental study: *Chemical Geology*, v. 354, p. 233–242, <https://doi.org/10.1016/j.chemgeo.2013.06.007>.
- Wolfe, E.W., Garcis, M.O., Jackson, D.B., Koyagani, R.Y., Neal, C.A., and Okamura, A.T., 1987, The Puu Oo eruption at Kilauea, episodes 1–20, January 3, 1983, to June 8, 1984, in Decker, R.W., Wright, T.L., and Stauffer, P.H., eds., *Volcanism in Hawaii: U.S. Geological Survey Professional Paper 1350*, p. 471–508, <https://doi.org/10.3133/pp1463>.
- Wright, R., and Flynn, L.P., 2003, On the retrieval of lava-flow surface temperatures from infrared satellite data: *Geology*, v. 31, p. 893–896, <https://doi.org/10.1130/G19645.1>.
- Yokota, T., García Mateo, C., and Bhadeshia, H.K.D.H., 2004, Formation of nanostructured steels by phase transformation: *Scripta Materialia*, v. 51, p. 767–770, <https://doi.org/10.1016/j.scriptamat.2004.06.006>.

Printed in USA